PCCP

Accepted Manuscript

ROYAL SOCIETY OF CHEMISTRY

www.rsc.org/pccp

Journal Name

RSCPublishing

ARTICLE

Physicochemical properties of *N*-propyl-*N*-methylpyrrolidinium bis(fluorosulfonyl)imide for sodium metal battery applications

Cite this: DOI: 10.1039/x0xx00000x

Received 00th January 2012,
Accepted 00th January 2012

DOI: 10.1039/x0xx00000x

www.rsc.org/

Hyungook Yoon[a,b], Haijin Zhu[a], Aziliz Hervault[a], Michel Armand[a,c], Douglas R. MacFarlane [b], and Maria Forsyth[a]

The physicochemical properties of a range of $NaNTf_2$ (or NaTFSI) salt concentrations in *N*-propyl-*N*-methylpyrrolidinium bis(fluorosulfonyl)imide (or C_3mpyrFSI) ionic liquid were investigated by DSC, conductivity, cyclic voltammetry and diffusivity. Cyclic voltammetry indicated a stable sodium plating behavior with a current of 5 $mA.cm^{-2}$ at 25 ^oC to 20 $mA.cm^{-2}$ at 100 ^oC, along with high reversibility identifying this electrolyte as a possible candidate for a sodium-ion or sodium metal battery applications. ^{23}Na NMR chemical shifts and spectral linewidths (FWHM) indicate a complex coordination of the Na+ ion which is dependent on both temperature and salt concentration with an apparently stronger coordination to the NTf2 anion with increasing $NaNTf_2$ concentration. Temperature dependent PFG-NMR diffusion measurements show that both FSI and NTf_2 have comparable behaviour although the smaller FSI anion is more diffusive.

Introduction

The lithium-ion battery technology has become the most successfully commercialized mobile energy storage device nowadays from the use of small sized applications such as wearable computing to the larger, smart grid energy storage uses.[1, 2] However, the share of lithium-ion battery technology in transportation is still very limited due to its high cost and limited driving range[3] and expansion of this technology to large scale stationary energy storage would lead to a ultimate shortfall in available lithium resources. Therefore, research efforts seeking an alternative electric storage system for low cost and high capacity, with reliable performance have become important. Therefore, the sodium-ion battery technology, whose mechanism should intrinsically be the same as for the lithium-ion analogue, has gained intensive interest due to the abundance of sodium and possible cost reduction.[4-7] A number of publications have recently appeared relating in particular to Na intercalating cathode materials[7-10] and anode materials.[4]

Along with the main efforts to find optimal electrode materials, identification of a suitable electrolyte which enables stable sodium cycling is also important, especially because the larger and heavier sodium ionic size may result in relatively lower diffusivity than the lithium ion.[11, 12] This relatively lower diffusivity combined with a higher redox potential of the Na/Na^+ couple[13] leads to a sodium ion battery having lower energy density, both theoretically and practically, until now.[14, 15] Contrary to lithium, sodium does not intercalate into graphite but does intercalate into hard carbon, although it is much inferior in terms of specific capacity and specific gravity.[13] Thus the prospect of using a sodium metal anode is interesting. The electrochemistry of sodium metal in ionic liquids has been investigated by Wibowo, et al. and other groups previously, showing that the thermodynamic electrochemical potential of sodium is electrolyte-specific and can approach that of lithium metal.[16-18] This indicates that a sodium 'metal' battery could potentially have a terminal voltage similar to that of traditional lithium batteries if a suitable high voltage Na intercalating cathode is found.

Most research published thus far using sodium metal as the anode in a Na device, have used propylene carbonate based electrolytes, the most promising being PC-FEC.[7] Slater, et al. also demonstrated a $Na_{0.6}Li_{0.6}Ni_{0.25}Mn_{0.75}O_y$ cathode showing 200 $mAh.g^{-1}$ reversible capacity at 4.8V charging with a PC based electrolyte.[13] However, carbonate based electrolytes cause corrosion of the sodium metal anode, which resulted in unstable cycling performances.[13] To avoid this problem, ionic liquid-based electrolytes for sodium metal anode have been investigated with the additional benefit of improved safety characteristics compared with organic electrolytes.[19, 20] Fukunaga, et al. reported a NaFSI-KFSI eutectic melt ionic liquid system for use as the electrolyte in sodium secondary batteries.[21] Ding, et al. demonstrated a sodium ion battery with 0.8 $mol.kg^{-1}$ NaFSI in C_3mpyrFSI.[22] A surprising result was also reported by Chagas et al. recently, which demonstrated a lab synthesized $Na_{0.45}Ni_{0.22}Co_{0.11}Mn_{0.66}O_2$ with a sodium metal anode having over 200 $mAh.g^{-1}$ in the 4.6V – 1.5V voltage range, with $NaNTf_2$ in C_4mpyrFSI.[11] In comparison with a carbonate-based electrolyte, this ionic liquid based electrolyte showed much better cycling ability. They rationalized the reason why the ionic liquid based electrolyte showed superior cycling stability compared with the PC based electrolyte was related to the cathode structure,[11] but we also postulate that the IL-based system has an additional beneficial effect on the Na anode, in part by inhibiting the corrosion reactions. Monti and Johansson have focused on the more fundamental properties of

this class of electrolyte by considering an imidazolium NTf_2 ionic liquid with added $NaNTf_2$ salt.[12] They report that, the coordination for sodium in the NTf_2 based electrolyte is different from the known solvation chemistry of the lithium ion in the NTf_2 or FSI based ionic liquid electrolyte, with 6-fold coordination by 3 anionic entities.[12, 23, 24] Our group has also previously demonstrated the salt concentration effect on the coordination and battery performance in lithium based systems, showing fast lithium ion transport in FSI based electrolytes,[25, 26] Similar behavior was also presented in an ether based FSI electrolyte by Yamada, et al.[27]
In this paper, we investigate the concentration dependence of the physical and electrochemical properties for $NaNTf_2$ in C_3mpyrFSI ionic liquid which has been shown to be a potential candidate for the sodium battery electrolyte. In particular we use conductivity and NMR spectroscopy to study the transport and structural behavior in these electrolytes, and demonstrate stable cycling of Na, even at elevated temperatures.

Experimental

C_3mpyrFSI (99%) was obtained from Suzhou Fluorite co. ltd. and $NaNTf_2$ (99.9%) were obtained from Solvionics™. These materials were used without further purification. The water content of C_3mpyrFSI was 28ppm, as determined by Karl Fischer titration (Metrohm™). Since initial solubility tests showed that $NaNTf_2$ can dissolve up to 1.35 mol.kg^{-1} in C_3mpyrFSI at 70 ^oC, we prepared five different samples ranging from 0.25 to 1.35 mol.kg^{-1}. However, a few weeks after the preparation of the 1.35 mol.kg^{-1} $NaNTf_2$ electrolyte, some sodium salt reprecipitated in the IL at 25 ^oC. Thus the actual solubility limit is likely to be a bit lower than 1.35 mol.kg^{-1} and the data presented here for this concentration is for a metastable system.

Differential scanning calorimetry (DSC) was carried out on Mettler Toledo DSC 1 with Mettler StareDB (ver. 10.00) software. DSC Samples (~10 mg) were sealed in Al hermetic pans and lids and then were cooled by liquid nitrogen at 20 $^oC.min^{-1}$ to -120 ^oC then the DSC traces were recorded during heating at 10 $^oC.min^{-1}$ to 60 ^oC.

Ionic conductivity was measured with a sealed glass conductivity dip-cell equipped with two platinized platinum electrodes; all preparations took place inside an Ar-filled glove box and the moisture contents were determined again after the conductivity measurement. A 0.01 M KCl solution was used to calibrate the cell before and after each sample measurement. The ionic conductivity was measured from 0 to 120 ^oC and then back to 30 ^oC in 10 ^oC steps to check for any hysteresis.

A 1.5 mm diameter Ni working electrode and an Ag wire counter electrode were employed for cyclic voltammetry. The reference electrode consisted of a silver wire immersed in a solution of 10 mM $AgNTf_2$ (99.95+% Solvonic™) in N-butyl-N-methylpyrrolidinium bis(trifluoromethanesulfonyl)imide (C_4mpyrNTf_2, 99%, 125 ppm of water, Merck) and separated from the main solution by a glass frit, as reported by us[28] or Snook et al..[29] Therefore, the CV measurements were performed against Ag | $AgNTf_2$ reference potential, then the potential was checked with a Fc | Fc^+ internal reference. The scan rate was 20 mV.s^{-1}. Potentiostatic control was provided by Biologic SP-200 controlled with EC-Lab (ver. 10.32) software.
All the NMR experiments were carried out on a Bruker Avance III 500 MHz wide bore spectrometer (with proton Larmor frequency of 500.07 MHz) equipped with a 5mm diff50 pulse-field gradient probe. Each sample was packed to a height of 50mm in a 5mm Schott E NMR tube in an Ar filled glove box and sealed with Teflon tape and a cap. The ^1H, ^{19}F NMR signals were used for the determination of the diffusion coefficients of the cation and anion species, respectively. The pulsed-field gradient stimulated echo (PFG-STE) pulse sequence[30] was used to obtain the diffusion coefficients of different species. ^{23}Na chemical shifts were obtained from single pulse excitation (SPE) experiments with a recycle delay of 10s. The maximum strength of our gradient amplifier was 29.454 T.m^{-1}. Each sample was measured from 0 ^oC – 70 ^oC. The sample temperatures for the variable temperature experiments were calibrated by using the relative chemical shift separation between the OH resonance and CH_3 resonance in dry methanol.[31]

Results and Discussion

Figure 1(a) shows the DSC traces of the neat C_3mpyrFSI IL. The melting transition can be clearly seen at -9 ^oC. Two additional solid-solid transitions, before the melting point, are detected at -19 ^oC and -82 ^oC. As previously reported,[32] the pure IL C_3mpyrFSI does not exhibit a glass transition in this temperature range and seems to crystallize immediately.

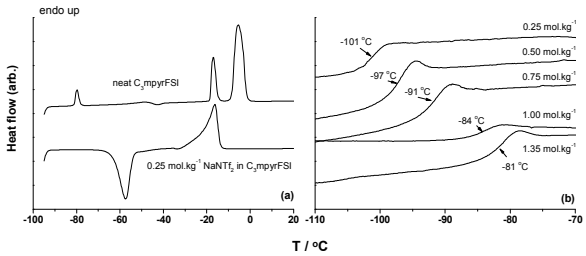

Figure 1 DSC traces of $NaNTf_2$ in C_3mpyrFSI electrolyte.

With addition of 0.25 mol.kg^{-1} $NaNTf_2$, we observe the appearance of a crystallization peak at -64 ^oC and the melting point is now detected at -31 ^oC. However, a glass transition is also observed at -101°C at this salt concentration. The crystallization and melting peaks completely disappear when the sodium salt concentration rises above 0.25 mol.kg^{-1} and only a glass transition is observed as shown in figure 1(b). This implies that crystallization has been disrupted by interactions between the sodium ions and the anions in the system at concentrations $\geq$ 0.25 mol.kg^{-1}. Moreover, the glass transition temperature (midpoint) increases with an increasing salt content from -101 ^oC for 0.25 mol.kg^{-1} to -81 ^oC for 1.35 mol.kg^{-1}, which is further evidence of interactions.

The electrical properties of the electrolytes have been characterized by conductivity measurements and plotted in figure 2.

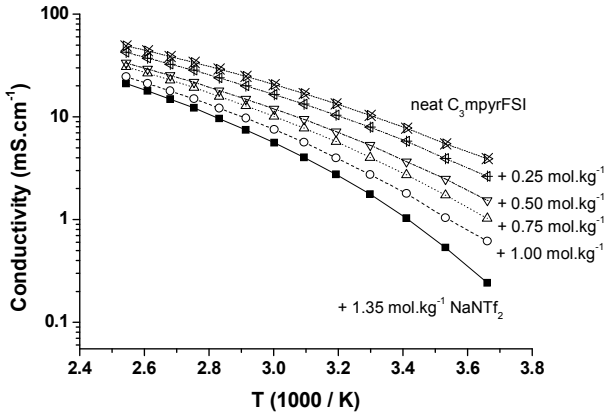

Figure 2 Arrhenius plot of the ionic conductivity of C_3mpyrFSI electrolyte with various concentrations of $NaNTf_2$ salt.

The measured ionic conductivity of neat C_3mpyrFSI at 25 °C is concordant with the previously reported value.[26, 33-39] The ionic conductivity decreases with increasing salt content. Several studies have reported that the conductivity values of an ionic liquid decrease with increasing sodium or lithium salt concentration, as a result of the increased viscosity.[25, 40, 41] The increase in viscosity is most likely the consequence of changes in speciation with large $[MX_n]^{(n-1)-}$ clusters being formed.

The ionic conductivity increases with increasing temperature as the fluidity increases. Moreover, ion pairs or ion clusters have enough energy to dissociate, and hence less energy is required for ion mobility.[41] The plots show curvature, and could be fitted well with the Vogel-Tamman-Fulcher (VTF) equation,[42]

$$\sigma = \sigma_0 \exp[-B/(T-T_0)]$$

where σ is the conductivity ($S.cm^{-1}$), T is the temperature (K), and σ_0 ($S.cm^{-1}$), B (K) and T_0 (K) are the fitting parameters. The calculated VTF parameters are listed in Table 1. The pre-exponent, σ_0 can been related to the number of charge carriers in an electrolyte system; B is often referred to as the pseudo-activation energy for ion transport; and T_0 is taken as the temperature at which the free volume disappears or the configurational entropy in the electrolyte system approaches zero.[43] The Adam-Gibbs configurational entropy model predicts T_0 to be near the glass transition temperature of the electrolyte and is found to be between 20 and 50°C below the measured T_g or ≈ 0.75 T_g.[44]

Table 1 VTF parameters for the ionic conductivity

	$NaNTf_2$ concentration in the IL ($mol.kg^{-1}$)					
	0	0.25	0.50	0.75	1.00	1.35
σ_0 ($mS.cm^{-1}$)	707 ±22	818 ±54	711 ±35	718 ±34	585 ±28	598 ±26
B (K^{-1})	653 ±12	735 ±27	730 ±19	725 ±18	700 ±17	706 ±15
T_0 (K)	149 ±2	145 ±4	154 ±3	163 ±2	171 ±2	182 ±2
T_0 (°C)	-124	-128	-119	-109	-101	-90
Tg (°C)	-	-101	-97	-91	-84	-81

In this system, for all samples containing the Na salt, the T_0 parameter is close to the experimental T_g values detected using the DSC technique, increasing with an increasing salt content due to the stronger ionic interactions in the presence of Na^+ ions in ratio. The B parameter (which can be thought of as a pseudo activation energy) of the neat IL is smaller than the B parameters of the Na^+ containing samples. Indeed, since ionic interactions are stronger between sodium cations and the anions within the electrolyte, more energy is needed for ion mobility. Interestingly, the value of B does not have a significant dependence on sodium ion concentration.

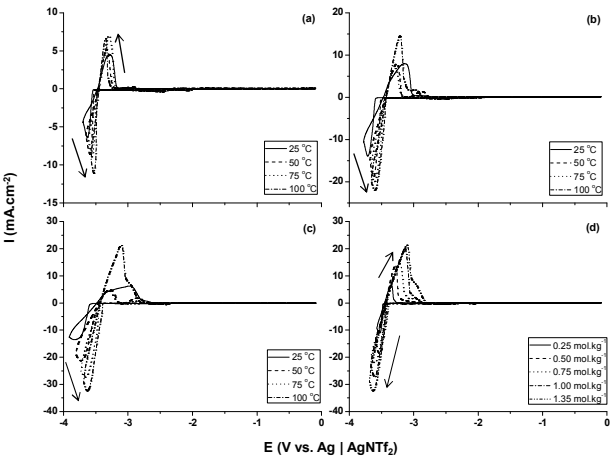

Figure 3 Cyclic Voltammograms of $NaNTf_2$ in C_3mpyrFSI electrolyte over a range of concentrations and temperatures; (a) 0.25 $mol.kg^{-1}$, (b) 0.75 $mol.kg^{-1}$, (c) 1.35 $mol.kg^{-1}$, and (d) at 100 °C. Ni working electrode

Figure 3(a) presents the temperature dependence of the cyclic voltammetry of a Ni electrode in 0.25 $mol.kg^{-1}$ $NaNTf_2$ in C_3mpyrFSI. Clear Na deposition and stripping features are observed indicating good cycling of the Na in this electrolyte at currents in excess of $20mA.cm^{-2}$ under certain conditions. As the temperature increases, both deposition and stripping currents increase as the arrows indicate. However, no significant peak differences are observed between the voltammograms obtained at different temperatures in this concentration. When the salt concentration increases to 0.75 $mol.kg^{-1}$, figure 3(b), and still further to 1.35 $mol.kg^{-1}$, figure 3(c), a second distinct stripping peak is found at -3V. Since it is known that a Ni working electrode does not form an alloy with sodium metal, it is not clear if this peak which appears at high salt concentration may be related to the NTf_2 anion or a possible configurational difference which is related with high Na salt which was shown in the similar system with Li salt.[25-27] This behavior is currently not fully understood and needs to be studied further.

The efficiency of the first cycle is around 40% to 60% and decreased to 30% beyond cycle 5. We also note that the cycling efficiency in this system varies hugely with small variations in the water content. When the water is lowered to < 10 ppm, almost 90% cycling efficiency was shown at 25 °C; however when the electrolyte contains more than 300 ppm water, almost no stripping peak was observed. Therefore, the recent report by Ding, et al,[22] with a similar system, which postulates low Na cycling efficiency due to the Ni working electrode,[22] may be more likely due to possible water contamination. Figure 3(d) shows the concentration dependence at 100 °C. The stripping peak current increases with the salt concentration, but the difference between 1.00 $mol.kg^{-1}$ and 1.35 $mol.kg^{-1}$ of $NaNTf_2$ is small. At the lower temperatures, the maximum peak current is observed for $NaNTf_2$ concentrations between 0.75 $mol.kg^{-1}$ and 1.00 $mol.kg^{-1}$ and this can be considered the optimum range for a sodium battery using this electrolyte.

The PFG-STE NMR experiments were performed for ^{19}F and ^{1}H for detecting the anions (FSI and NTf_2) and the cations (C_3mpyr), respectively and the diffusion coefficients of the ions for each electrolyte composition are displayed in figure 4(a). We note that obtaining the ^{23}Na diffusion coefficient was not possible under the present conditions because T_2 for the sodium is too short to carry out the measurements.

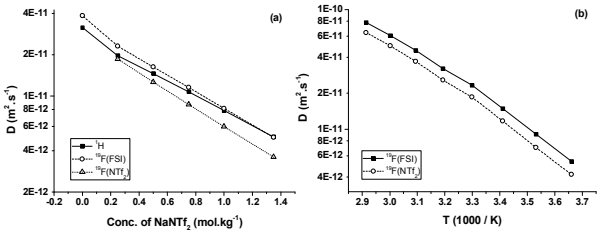

Figure 4 Diffusion coefficients (a) of the different ions with the salt concentrations, (b) as a function of temperature in the 0.5 mol.kg^{-1} $NaNTf_2$

The diffusion coefficients decrease with an increasing salt content, likely due to the increasing viscosity of the solution (thus decreasing ion mobility). However, the diffusion coefficient of the two anions seems to decrease faster than the diffusion coefficient of the IL cation for high salt concentrations. One possibility for this different behaviour is that, whilst the cation will most certainly take part in the ionic clusters that form between Na^+ and the two anions, the interactions will be weaker or more diffuse than the Na-FSI or Na-NTf_2 interactions. Thus the effect of the Na^+ addition is not as dramatic on the average diffusion coefficient of the pyrrolidinium cation. The diffusion coefficients of the two anions (FSI and NTf_2) in 0.5 mol.kg^{-1} $NaNTf_2$ containing electrolyte were measured between 0 ^oC and 70 ^oC in figure 4(b). According to these results, the two anions seem to behave similarly over this range of temperature, although the FSI anion diffuses faster than the NTf_2 anion because it is smaller. Figure 4 (a) shows that, with increasing NTf_2 concentration, the diffusion coefficient of both FSI and NTf_2 anions decrease and have a similar concentration dependency. This likely suggests a fast exchange between the FSI and NTf_2 in the ion clusters and indeed, the ion clusters are unlikely to contain only FSI or NTf_2 but rather they will contain a mixture of both anion species (in addition of course to the cations). These fast exchange process exists not only between various ionic clusters but also between these clusters and individual 'free' or dissociated ions. The experimental diffusion coefficient of any given ion, FSI for example, is a number-averaged value of all the species (individual ions, ion pairs, triples and larger aggregates for example). The same is true for the NTf_2 anions. Since free FSI ions are smaller, they will diffuse more rapidly than the larger, free NTf_2 anion, even though the associated ion moving in any given cluster will have the same diffusion coefficient. Therefore, on average, the smaller FSI anion will have an apparent diffusion coefficient that is systematically higher than that of the NTf_2, with the concentration dependence of both anions being similar. The fact that this difference is observed also suggests the rapid exchange of ions between various species.

Figure 5 shows ^{23}Na chemical shifts for each electrolyte composition between 0 ^oC – 70 ^oC temperature range.

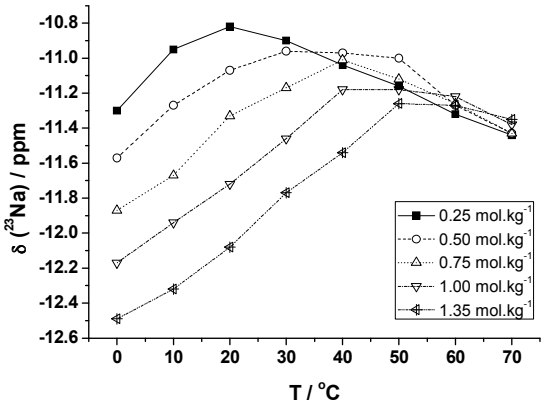

Figure 5 ^{23}Na chemical shifts as a function of temperature.

The ^{23}Na chemical shifts change as function of both salt concentration and temperature. A high sodium salt concentration causes an upfield chemical shift (increasing magnetic shielding). Increasing the temperature leads to an increase of the chemical shift until a maximum is reached, and beyond this temperature all samples show the same behavior with the chemical shifts of the different electrolytes overlapping, independent of the composition. According to these results, we hypothesize that:

- For the most dilute electrolytes, there are more FSI anions in the first coordination shell of Na than NTf_2 ions.
- By increasing the concentration of $NaNTf_2$ salt, the NTf_2 concentration also increases and thus there is increasing competition between the two anions to coordinate to the sodium cation; thus the chemical environment consists of a mixture of the two anions which may undergo rapid exchange between species. In the case of Li-NTf_2, the coordination number was lower than for Li complexes with FSI.[45] This may also be true in the case of sodium since the NTf_2 anion is bulkier than the FSI anion and thus this difference likely arises from steric effects. According to a previous study,[12] the Na^+ ion is coordinated by 6 oxygen atoms and its energetically preferred structure is $[Na(NTf_2)_3]^{2-}$, which means that NTf_2 anions chelate the sodium ion. Therefore, Na-NTf_2 interactions are stronger than Na-FSI interactions which results in a greater shielding and thus a more negative chemical shift value.
- The increasing temperature weakens the ionic interactions and therefore lessens the electron shielding effect from the anions. As a result, the ^{23}Na cation becomes more positively charged and hence the chemical shift is less negative. Interestingly, the temperature at which the chemical shift reached a maximum increased with increasing salt content. This appears to correlate with the increasing Tg of these systems, which reflects a lower mobility at any given temperature. If the changes in chemical shift reflect a changing in the chemical environment (eg. different chemical complexes involving clusters of Na, FSI and NTf_2 in equilibrium with one another) ion exchange kinetics will be slower for systems with higher Tg. The maximum is thought to reflect a point where the essential environment of the Na ions is the same independent of concentration.
- The reason for the overlapping of the chemical shifts at high temperature, independent of concentration, may be due to fast anion exchange around Na; interactions are weaker, and there is rapid exchange between the different possible Na coordination environments (resulting, on average, in Na experiencing all possible

coordination spheres) and the chemical shift is now independent of the system composition.

The full width half maximum frequency (Δν) of a ^{23}Na peak which is shown in figure 6 is inversely related to the T_2 relaxation time. Therefore, a rapid relaxation will lead to a line broadening. The relaxation time is mainly influenced by the atom mobility and site exchange velocity.

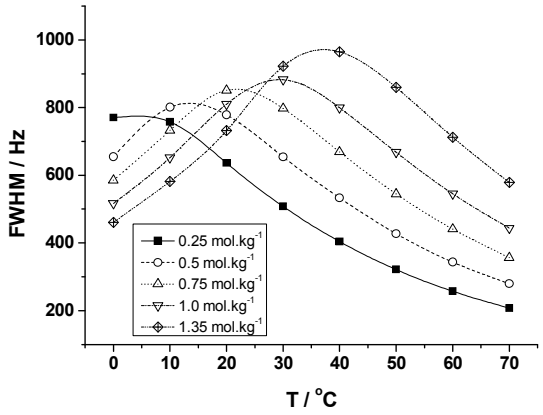

Figure 6 Full width half maximum frequencies of the ^{23}Na NMR spectra as a function of temperature

For each electrolyte composition, two regions are observed. Firstly an increase of Δν is observed with increasing temperature in the low temperature range, which is most likely related to an exchange broadening mechanism as a result of rapid site exchange detectable in the time scale of the NMR acquisition (a few ms). On the other hand, in the higher temperature region, a decrease of the FWHM is observed with increasing temperature which is due to motion induced line narrowing, with the increasing mobility of the ions averaging out all the interactions which lead to line broadening. As with the chemical shift data, the maximum Δν is shifted toward higher temperatures when the salt concentration is raised, again reflecting the higher T_g and slower exchange kinetics between different possible species. These results are thus consistent with the hypotheses deduced from the ^{23}Na chemical shift data.

Conclusions

The diffusion behaviors, ionic conductivities, thermal and electrochemical properties of $NaNTf_2$-based C_3mpyrFSI electrolytes were investigated. No glass transition was detected for the neat IL, but only a melting point at -9 °C which is no longer apparent when the salt concentration is raised above 0.25 mol.kg^{-1} while the glass transition temperature increases from -101°C to nearly -80°C when the salt concentration increases. The conductivity behavior of the system was well described by the VTF equation, although the pseudo activation energy parameter B is not significantly changed with the addition of increasing $NaNTf_2$ salt. The increase of the glass transition temperature and the decrease of the conductivity with increasing salt content are consistent with the appearance of ionic interactions (ion pairs/clusters) between the sodium cation and the FSI and NTf_2 anions which is also consistent with the ^{23}Na NMR data. The cyclic voltammetry experiments have shown that the sodium can be cycled in this mixed electrolyte in a wide temperature range from 25 °C to 100 °C. Elevated temperature and increased salt concentrations seem to facilitate the sodium deposition reaction, with an optimum concentration range at a given temperature. The diffusion coefficients of the different ions composing the electrolyte decrease with increasing salt content, as would be expected from the increasing T_g. The two anions show the same diffusion trends with temperature, although the average mobility FSI is greater than NTf_2 owing to its smaller size. The ^{23}Na NMR data provides evidence of a more mixed chemical environment in the more concentrated electrolyte with several types of coordination environments possible for the Na cation and fast anion exchange in the sodium ion coordination sphere apparent. Additional experiments are underway in the systems with homologous anions to investigate this exchange phenomenon.

Since $NaNTf_2$ doped C_3mpyrFSI systems may overcome the safety problems associated with sodium metal and conventional electrolytes and still exhibit good conductivities and stabilities, we conclude that they are very promising as electrolytes for Na secondary batteries operating at low temperature.

Acknowledgements

We thank the ARC (Australian Research Council) for funding through DP130101652. MF and DRM acknowledge their ARC Laureate fellowships. MA gratefully acknowledges Deakin University for travel funding through the "Thinker in Residence" program.

Notes and references

[a] ARC Centre of Excellence for Electromaterials Science (ACES), Institute for Frontier Materials (IFM), Deakin University, Burwood, Victoria 3125, Australia

[b] School of Chemistry, Monash University, 3800 Victoria, Australia

[c] CIC energigune, Alava Technology Park, Albert Einstein 48 - 01510 Miñano, Álava, Spain

Electronic Supplementary Information (ESI) available: [details of any supplementary information available should be included here]. See DOI: 10.1039/b000000x/

1. M. S. Whittingham, *Proceedings of the IEEE*, 2012, **100**, 1518-1534.
2. S.-Y. Lee, K.-H. Choi, W.-S. Choi, Y. H. Kwon, H.-R. Jung, H.-C. Shin and J. Y. Kim, *Energy & Environmental Science*, 2013, **6**, 2414-2423.
3. J. B. Goodenough, *Journal of Solid State Electrochemistry*, 2012, **16**, 2019-2029.
4. S. Komaba, W. Murata, T. Ishikawa, N. Yabuuchi, T. Ozeki, T. Nakayama, A. Ogata, K. Gotoh and K. Fujiwara, *Adv. Funct. Mater.*, 2011, **21**, 3859-3867.
5. J. B. Goodenough, *Accounts Chem. Res.*, 2013, **46**, 1053-1061.
6. S. P. Ong, V. L. Chevrier, G. Hautier, A. Jain, C. Moore, S. Kim, X. Ma and G. Ceder, *Energy and Environmental Science*, 2011, **4**, 3680-3688.
7. S.-M. Oh, S.-T. Myung, J. Hassoun, B. Scrosati and Y.-K. Sun, *Electrochemistry Communications*, 2012, **22**, 149-152.
8. S. Kim, X. Ma, S. P. Ong and G. Ceder, *Physical Chemistry Chemical Physics*, 2012, **14**, 15571-15578.

9. L. Wang, Y. Lu, J. Liu, M. Xu, J. Cheng, D. Zhang and J. B. Goodenough, *Angewandte Chemie - International Edition*, 2013, **52**, 1964-1967.
10. M. Xu, L. Wang, X. Zhao, J. Song, H. Xie, Y. Lu and J. B. Goodenough, *Physical Chemistry Chemical Physics*, 2013, **15**, 13032-13037.
11. L. G. Chagas, D. Buchholz, L. Wu, B. Vortmann and S. Passerini, *Journal of Power Sources*, 2014, **247**, 377-383.
12. D. Monti, E. Jónsson, M. R. Palacín and P. Johansson, *Journal of Power Sources*, 2014, **245**, 630-636.
13. M. D. Slater, D. Kim, E. Lee and C. S. Johnson, *Adv. Funct. Mater.*, 2013, **23**, 947-958.
14. S. W. Kim, D. H. Seo, X. Ma, G. Ceder and K. Kang, *Advanced Energy Materials*, 2012, **2**, 710-721.
15. B. L. Ellis and L. F. Nazar, *Current Opinion in Solid State and Materials Science*, 2012, **16**, 168-177.
16. R. Wibowo, L. Aldous, E. I. Rogers, S. E. Ward Jones and R. G. Compton, *Journal of Physical Chemistry C*, 2010, **114**, 3618-3626.
17. R. Wibowo, L. Aldous, S. E. W. Jones and R. G. Compton, *Chemical Physics Letters*, 2010, **492**, 276-280.
18. J. A. Vega, J. Zhou and P. A. Kohl, *Journal of the Electrochemical Society*, 2009, **156**, A253-A259.
19. H. Ohno, in *Electrochemical Aspects of Ionic Liquids*, ed. O. Hiroyuki, 2005, pp. 1-3.
20. H. Sakaebe, H. Matsumoto and K. Tatsumi, *Electrochimica Acta*, 2007, **53**, 1048-1054.
21. A. Fukunaga, T. Nohira, Y. Kozawa, R. Hagiwara, S. Sakai, K. Nitta and S. Inazawa, *Journal of Power Sources*, 2012, **209**, 52-56.
22. C. Ding, T. Nohira, K. Kuroda, R. Hagiwara, A. Fukunaga, S. Sakai, K. Nitta and S. Inazawa, *Journal of Power Sources*, 2013, **238**, 296-300.
23. K. Fujii, T. Fujimori, T. Takamuku, R. Kanzaki, Y. Umebayashi and S. I. Ishiguro, *Journal of Physical Chemistry B*, 2006, **110**, 8179-8183.
24. K. Fujii, S. Seki, S. Fukuda, R. Kanzaki, T. Takamuku, Y. Ulmebayashi and S.-i. Ishiguro, *Journal of Physical Chemistry B*, 2007, **111**, 12829-12833.
25. H. Yoon, P. C. Howlett, A. S. Best, M. Forsyth and D. R. MacFarlane, *Journal of the Electrochemical Society*, 2013, **160**, A1629-A1637.
26. H. Yoon, A. S. Best, M. Forsyth, D. R. MacFarlane and P. C. Howlett, *Journal of Physical Chemistry C*, 2014, manuscript submitted.
27. Y. Yamada, M. Yaegashi, T. Abe and A. Yamada, *Chemical Communications*, 2013, **49**, 11194-11196.
28. H. Yoon, G. H. Lane, Y. Shekibi, P. C. Howlett, M. Forsyth, A. S. Best and D. R. MacFarlane, *Energy & Environmental Science*, 2013, **6**, 979-986.
29. G. A. Snook, A. S. Best, A. G. Pandolfo and A. F. Hollenkamp, *Electrochem. Commun.*, 2006, **8**, 1405-1411.
30. R. M. Corns, M. J. R. Hoch, T. Sun and J. T. Markert, *Journal of Magnetic Resonance (1969)*, 1989, **83**, 252-266.
31. A. L. Van Geet, *Analytical Chemistry*, 1970, **42**, 679-680.
32. M. Kunze, S. Jeong, E. Paillard, M. Winter and S. Passerini, *Journal of Physical Chemistry C*, 2010, **114**, 12364-12369.
33. H. Matsumoto, H. Sakaebe, K. Tatsumi, M. Kikuta, E. Ishiko and M. Kono, *J. Power Sources*, 2006, **160**, 1308-1313.
34. A. Guerfi, S. Duchesne, Y. Kobayashi, A. Vijh and K. Zaghib, *J. Power Sources*, 2008, **175**, 866-873.
35. M. Ishikawa, T. Sugimoto, M. Kikuta, E. Ishiko and M. Kono, *J. Power Sources*, 2006, **162**, 658-662.
36. Y. Wang, K. Zaghib, A. Guerfi, F. F. C. Bazito, R. M. Torresi and J. R. Dahn, *Electrochim. Acta*, 2007, **52**, 6346-6352.
37. S. Seki, Y. Kobayashi, H. Miyashiro, Y. Ohno, Y. Mita, N. Terada, P. Charest, A. Guerfi and K. Zaghib, *J. Phys. Chem. C*, 2008, **112**, 16708-16713.
38. A. Guerfi, M. Dontigny, Y. Kobayashi, A. Vijh and K. Zaghib, *J. Solid State Electrochem.*, 2009, **13**, 1003-1014.
39. K. Hayamizu, S. Tsuzuki, S. Seki, K. Fujii, M. Suenaga and Y. Umebayashi, *Journal of Chemical Physics*, 2010, **133**.
40. G. H. Lane, P. M. Bayley, B. R. Clare, A. S. Best, D. R. MacFarlane, M. Forsyth and A. F. Hollenkamp, *Journal of Physical Chemistry C*, 2010, **114**, 21775-21785.
41. A. Andriola, K. Singh, J. Lewis and L. Yu, *Journal of Physical Chemistry B*, 2010, **114**, 11709-11714.
42. G. Y. Gu, R. Laura and K. M. Abraham, *Electrochemical and Solid-State Letters*, 1999, **2**, 486-489.
43. H. Ohno, M. Yoshizawa and T. Mizumo, in *Electrochemical Aspects of Ionic Liquids*, ed. O. Hiroyuki, 2005, pp. 75-81.
44. R. Richert and C. A. Angell, *Journal of Chemical Physics*, 1998, **108**, 9016-9026.
45. C. J. F. Solano, S. Jeremias, E. Paillard, D. Beljonne and R. Lazzaroni, *Journal of Chemical Physics*, 2013, **139**.